ARMY RESEARCH LABORATORY

Effect of Propellant Grain Dimensions on Progressivity

by Kevin J. White

ARL-TR-1532

October 1997

Approved for public release; distribution is unlimited.

Army Research Laboratory

Aberdeen Proving Ground, MD 21005-5066

ARL-TR-1532 **October 1997**

Effect of Propellant Grain Dimensions on Progressivity

Kevin J. White

Weapons and Materials Research Directorate, ARL

Abstract

For high loading density propelling charges, propellant grain geometry design is employed to improve ballistic efficiency. Specifically, grains that have 7 and 19 and even 37 perforations are used. These grains all have progressive geometries, i.e., surface areas that increase as the propellant burns. This report studies the effect of grain dimensions on progressivities of the 7- and 19-perforation geometries. Calculations show that for maximum progressivity, the ratio of grain diameter to perforation diameter should be as large as practical. It is shown that small values can degrade potential gun performance. Calculations also show that the grain length-to-diameter ratio should be at least between 1 and 2 for maximum progressivity. This effect is very nonlinear, and values less than 1 are shown to reduce progressivity and gun performance significantly. High-progressivity geometries have, however, an undesirable effect on ballistic temperature sensitivity and yield an increased sensitivity to propellant manufacturing variability.

ACKNOWLEDGMENTS

The author would like to thank F. Robbins, R. Anderson, A. Brant, and W. Oberle for their useful suggestions during the review of this report.

INTENTIONALLY LEFT BLANK.

TABLE OF CONTENTS

INTENTIONALLY LEFT BLANK.

LIST OF FIGURES

LIST OF TABLES

INTENTIONALLY LEFT BLANK.

1. INTRODUCTION

There is a strong interest within the military (both Army and Navy) in obtaining longer standoff distances in direct- and indirect-fire applications. Furthermore, with the current budgetary constraints these improvements need to be accomplished without obtaining a new weapons systems. Retrofitting with a new ammunition in existing systems will result in considerable savings. One of the straightforward ways of accomplishing this is by increasing muzzle velocity using either more propellant or a higher energy propellant (or both) in the existing gun chamber. In retrofitting, the same restrictions in the gun with respect to maximum operating pressure and acceleration still hold, along with the given projectile travel. The problem, then, with using the higher loading density/energy propellant is to safely ignite the charge and to operate in a ballistically efficient manner to extract the increased energy in the form of improved muzzle velocity. The increased energy is necessary, but the overall efficiency of the system must be maintained (or improved). Any decrease in efficiency would mean that the increased energy could not be *fully* exploited in terms of muzzle velocity.

To illustrate the problems that arise in attempting to accomplish this, a physical description of the interior ballistic process is given. In this way, a background is established for the study of propellant grain geometry, which is described in the following sections.

When the propellant in the gun chamber is ignited, the pressure rises and the projectile starts to move down the gun tube. The most efficient use of the propellant energy is for the pressure to rise as rapidly as possible to the maximum operating pressure and remain there until all the propellant is consumed. This is then followed by an isentropic expansion as the projectile moves to muzzle exit. As the projectile accelerates, the free volume in the chamber increases. In order for the pressure to remain at the maximum allowable value, the propellant mass generation rate must keep up with the rapidly increasing volume. The mass generation rate, dm/dt, is given by

$$dm/dt = \rho D A dx/dt, \tag{1}$$

where ρ is the density, A is the total propellant surface area, and dx/dt is the burn rate of the propellant. Since the density is nearly constant, the mass generation rate can be changed by altering A or dx/dt. The latter can be accomplished by formulating propellant compositions with variable burn rates (Robbins and Worrell 1992). A second way of increasing dm/dt at and after the maximum pressure is through A. Traditionally this is done by designing the propellant grain geometry so that the burning surface area will increase as the propellant combusts. Two important practical designs that give this increased surface area are the 7-perforation (perf) and the 19-perf grain geometries illustrated in Figure 1.

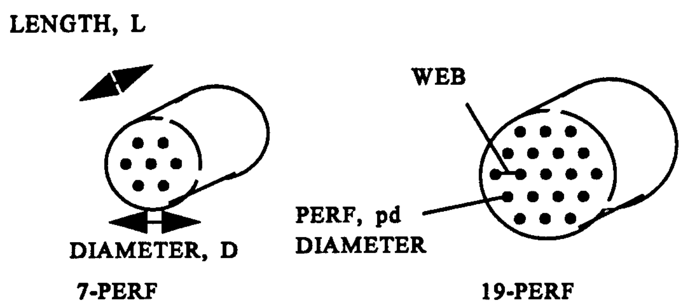

Figure 1. 7-perf (D = 3pd + 4web); 19-perf (D = 5pd + 6web).

In these cases, as the propellant burns, the outside surface decreases in area, but the perforation surface area increases. The ratio of the total reacting surface area to the initial surface area (the progressivity), as a function of the fraction of propellant burned, is illustrated in Figure 2. The maximum in the curve occurs when the web (defined in Figure 1) burns through and the remaining "slivers" burn in a regressive manner. In Figure 2 this occurs at a mass fraction of approximately 0.8. It would seem that the 19-perf geometry should always have a greater progressivity than the 7-perf geometry simply because there is a larger number of perforations that have an increasing area as the propellant burns. However, as is seen later, propellant design constraints either due to manufacturing limitations or propellant burn rate considerations, such as perf-augmented burning (Robbins and Horst 1983a, 1983b; Juhasz et al. 1984), may dictate geometries that do not take full advantage of the potential progressivity.

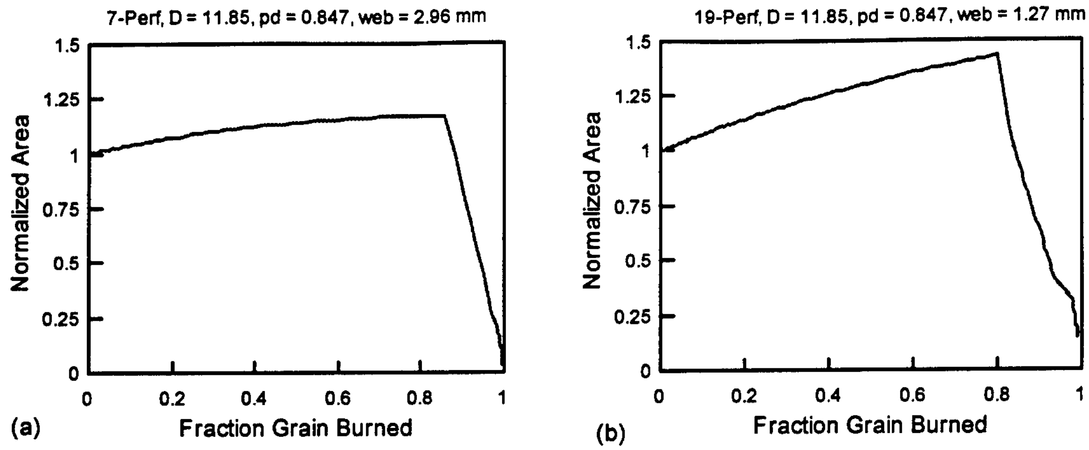

Figure 2. Progressivity, (a) 7-perf; (b) 19-perf grain geometry (L/D = 1.1).

Other problems can occur in the use of higher energy propellants or higher loading densities. (Further discussion is given in White et al. [1995].) These conditions result in contradictory requirements on mass generation rates. When the loading density is increased, the free volume in the chamber is reduced. This smaller free volume means that the mass generation rate, dm/dt, must be reduced in the early pressurization of the chamber so as not to exceed the maximum gun pressure. This is accomplished by reducing the initial propellant surface area (this assumes a uniform propellant composition). However, after the maximum pressure has been reached, dm/dt must be increased to keep up with the rapid increase in volume as the projectile moves down bore. Thus, as the loading density is increased, there is a need for even greater progressivity. When a new propellant that has a higher specific energy is used, similar problems are encountered as the initial surface area must be reduced to avoid excessive pressures. Furthermore, the problem may be complicated by the fact that newer higher energy propellants may have new *burn rates,* which can also cause further adjustments to the initial propellant surface area. These changes, as is shown later, can result in an unfavorable alteration in the grain progressivity.

Specifically, this problem was studied by Robbins, Keys, and Brant (to be published), when introducing a high-energy, slower-burning nitramine propellant formulation in a 120-mm cannon. In spite of the higher energy, the resultant calculated muzzle velocity was actually lower than for the conventional JA2 formulation. Using 19-perf grain geometry, it was found that the optimized web for the nitramine propellant resulted in a progressivity that was no better than a 7-perf granulation and considerably lower than the standard JA2 19-perf grain. Thus, the increased propellant energy could not be fully exploited in this particular case. The reason for this and other grain geometry effects on performance is discussed in the following sections. What is clear is that as propellant energies and loading densities are increased and burn rates altered, consideration of the effect of progressivity on the interior ballistics is required in order to fully exploit propellant advances for increased muzzle energy.

2. PROGRESSIVITY

As already discussed, the grain progressivity is defined as the burning area of a grain after a fraction burned divided by the original unburned grain area. Figure 3 shows a 7-perf grain with distance burned r; the shaded area represents the material burned (for clarity only 1 perf is shown burned). For purposes of simplicity, we only consider the progressivity up to slivering (i.e., to where r = web/2). All webs are assumed equal. Let "f" be the web fraction burned from ignition (r = 0) up to web/2 (i.e., the point where slivering begins). At this point the remaining slivers burn in a regressive manner. This is seen in Figure 2 where it can be shown that slivering occurs at fraction *grain* burned ≈ 0.8.

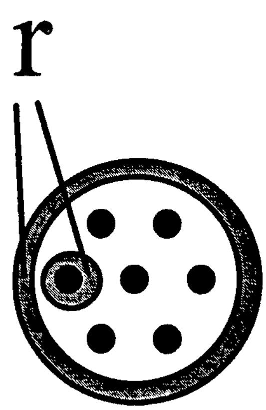

Figure 3. 7-perf (r = distance burned).

The grain surface area is divided up into three parts: the outside area (the lateral outside surface), the perf area (the area defined by the interior of the perforations), and the end area (the area at both ends of the grain). The areas of the burning surface are given by

$$A_o(\text{outside}) = \pi(D - 2r)(L - 2r), \tag{2}$$

$$A_p(\text{perforation}) = \pi(pd + 2r)(L-2r)n, \tag{3}$$

and

$$A_e(\text{ends}) = \pi/2[(D - 2r)^2 - n(pd + 2r)^2], \tag{4}$$

where r is the depth burned,

$$r = f(\text{fraction burned})x \text{ web}/2. \tag{5}$$

D is the outside diameter (Figure 1), r the distance burned, L the length, pd the perf diameter, and n the number of perfs. The web, D, and pd are related through the equations

$$D(\text{19-perf}) = 5pd + 6web \tag{6}$$

and

$$D(\text{7-perf}) = 3pd + 4web. \tag{7}$$

The progressivity, P, is defined as

$$P = [A_o(r) + A_p(r) + A_e(r)]/[A_o(0) + A_p(0) + A_e(0)]. \tag{8}$$

The surface area of the perforations is (for practical grains) progressive, but the outside and ends are regressive (Appendix A). An example of a 19-perf grain progressivity is shown in Figure 4, with nominal values for grain dimensions (D, 13 mm; pd, 0.8 mm; L/D, 1.1). Figure 4(a) gives the overall progressivity plotted against fraction burned (f) up to slivering. Figure 4(b) illustrates the contribution to the progressivity of the three surfaces: the perf (+), the outside (▲), and the end areas (■). The y-axis represents the percent *change* in area of each surface. The sum of all three gives the percent change in total surface area of the grain. It is seen that the perf area dominates the contribution as the grain burns, thus leading to the total area increase of approximately 50% when the web burns through at f = 1. Figure 4(c) illustrates the individual areas as a percentage of the total initial area (the grain area before combustion). At the start of burn (f = 0), it is seen that the perf area (+) and the outside areas (▲) are nearly the same, with the ends (■) being smaller. As the grain burns, the outside and ends decrease, but the perfs increase at a higher rate, resulting in an increase in total surface area. We will refer to these types of charts later as the effect of grain parameters on progressivity is investigated.

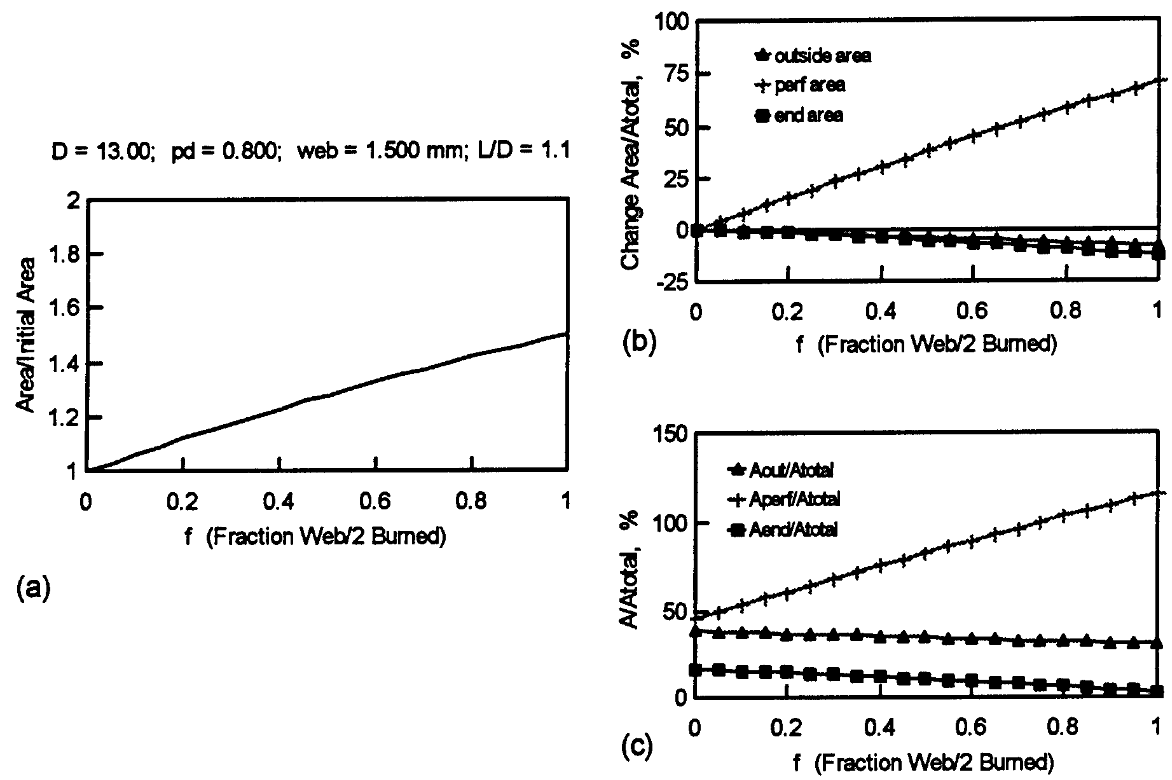

Figure 4. (a) Progressivity, 19-perf; (b) percent change in area; (c) areas, percent of original area.

2.1 Effect of D/pd on Progressivity. We have chosen this ratio as the first parameter to investigate. If the grain length is long compared with the diameter, the end areas can be neglected and the progressivity for a 19-perf grain can be written using equations 2–6 as

$$P_{19}(\text{approx.}) = 1 + 3f(D/pd - 5)/(D/pd + 19), \tag{9}$$

which depends only on the D/pd ratio. The actual value of the progressivity, including end effects, is plotted in Figures 5 and 6 for two cases. The perf diameter was chosen to be 0.8 mm with an outer diameter of 5 mm (D/pd = 6.25, Figure 5) and 15 mm (D/pd = 18.75, Figure 6). The L/D was chosen to be 100. The effect of the D/pd ratio is clearly seen. The reason for this can be understood from parts (b) and (c) for each figure. Parts (b) of the figures represent the partitioning of the total grain surface area between the perfs (+), outside (▲), and end (■) areas. As is evident, we have chosen a grain in which the end areas are insignificant. It is also seen that for the small grain (Figure 5), the bulk of the area comes from the perf area, whereas for the large grain (Figure 6) there is a near equal division between the perf area and the outside area. When the outside diameter is smaller, however, the area *change* is relatively small before the grain has burned through the web (Figure 5[b]). Note that the web for the 5-mm-diameter grain is 0.167 mm, and for the 15-mm grain it is 1.833 mm. The small web does not allow for a very large change in area, which results in a low progressivity. If, however, a very small perf diameter were chosen for the 5-mm-diameter grain, such that the D/pd ratio was increased to 18.75, the progressivity curve would be the same as that of the larger 15-mm-diameter grain. The web is still smaller than for the 15-mm grain, but now the percent *change* in perf area is increased, leading to a progressivity that is as large as the 15-mm grain. Examination of equation 9 reveals that the slope, 3(D/pd-5)/(D/pd+4), will vary from 0 to 3 when D/pd goes from a minimum value of 5 up to a large number. It is clear that to obtain the maximum progressivity, the largest practical D/pd should be used.

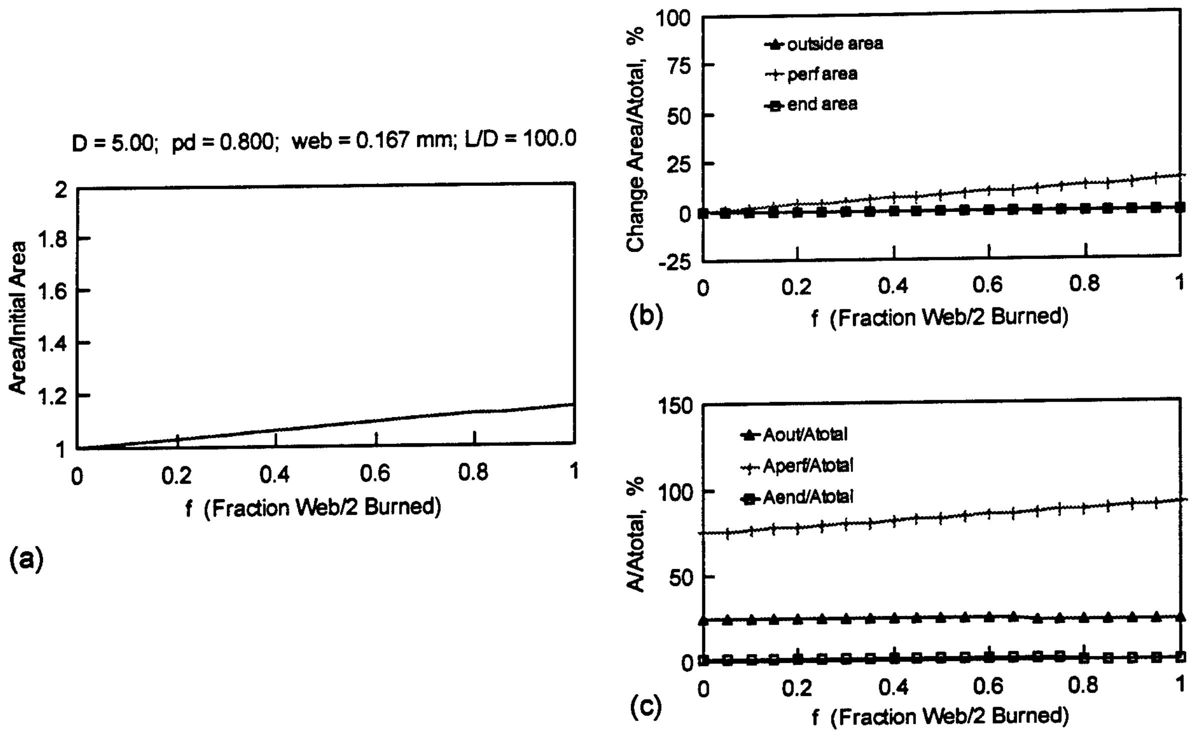

Figure 5. (a) Progressivity, 19-perf, D/pd = 6.25; (b) percent change in areas (■ and ▲ coincide); (c) areas, percent of original.

2.2 Effect of L/D on Progressivity. In the previous examples the grain was made intentionally long so as to be able to ignore end effects. However, as is seen from equation 4, the end areas are regressive in a nonlinear way, and when the grain web is a significant fraction of the length L, examination of equation 2 shows that the progressive rate of the perforation area is reduced as the grain burns down to slivers. This effect is illustrated in a comparison of Figures 7 and 8. In Figure 7, the D/pd ratio (18.75) is the same as that used in Figure 6 except that the L/D ratio is now 0.5 instead of 100. A distinct nonlinearity is observed in the perf area (+) function as the perforations become noticeably shorter when the grain burns. Additionally the regressive end areas (■) now make a significant contribution, with a reduction of surface area. This contributes to a significant reduction in progressivity as seen in Figure 7(a).

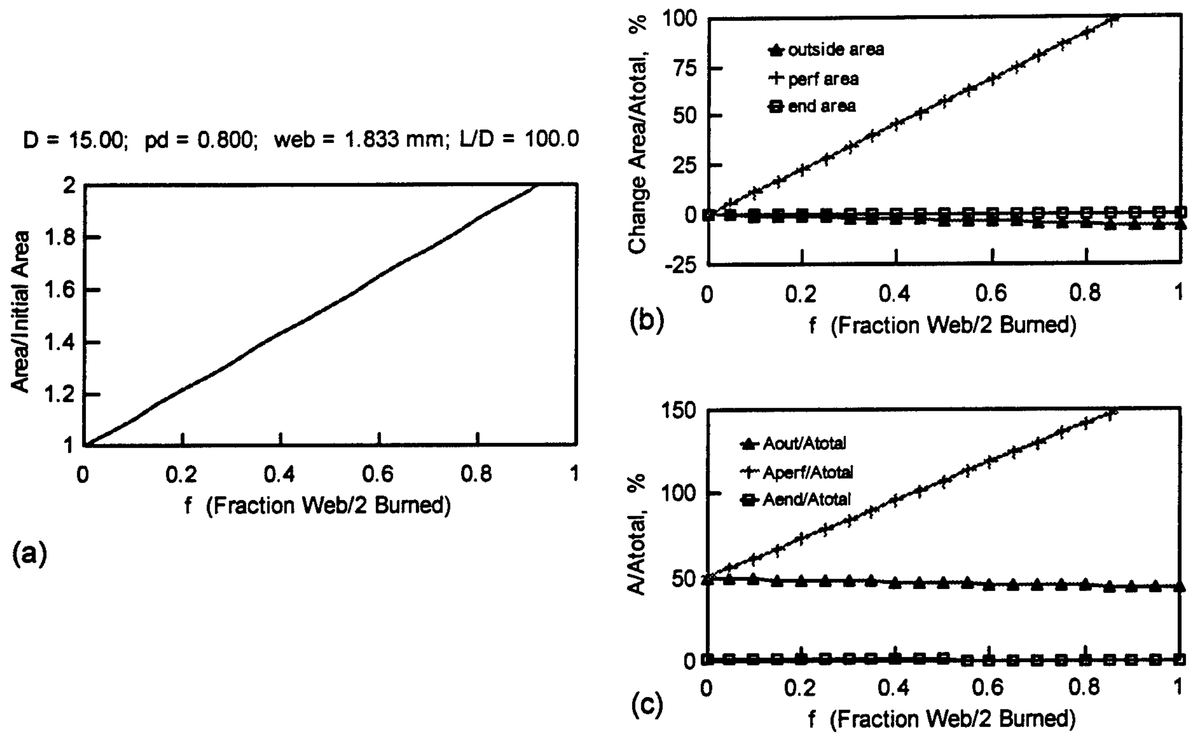

Figure 6. (a) Progressivity, 19-perf, D/pd = 18.75; (b) percent change in area; (c) areas, percent of original.

The effect of L/D is even more significant on the 7-perf grain geometry. Figure 8 shows the progressivity for L/D of 10 and Figure 9 for an L/D of 0.8. Because of the fewer number of perfs, the contribution of the end areas becomes more significant than for the 19-perf geometry.

3. DISCUSSION

From the results discussed previously it is clear that, except for cases where the L/D is small, the dependence of the progressivity on the fraction burned is nearly linear. As a consequence a reasonable figure of merit on progressivity is to evaluate the ratio of A(f)/A(0) at slivering (i.e., when f approaches 1.0). Table 1 evaluates the progressivity at f = 1 (slivering) for both the 7- and 19-perf geometries with a representative number of grain sizes. Also listed is the percent mass fraction burned at slivering. It is seen that the L/D should be greater than 1 or even as large as 2 in order to

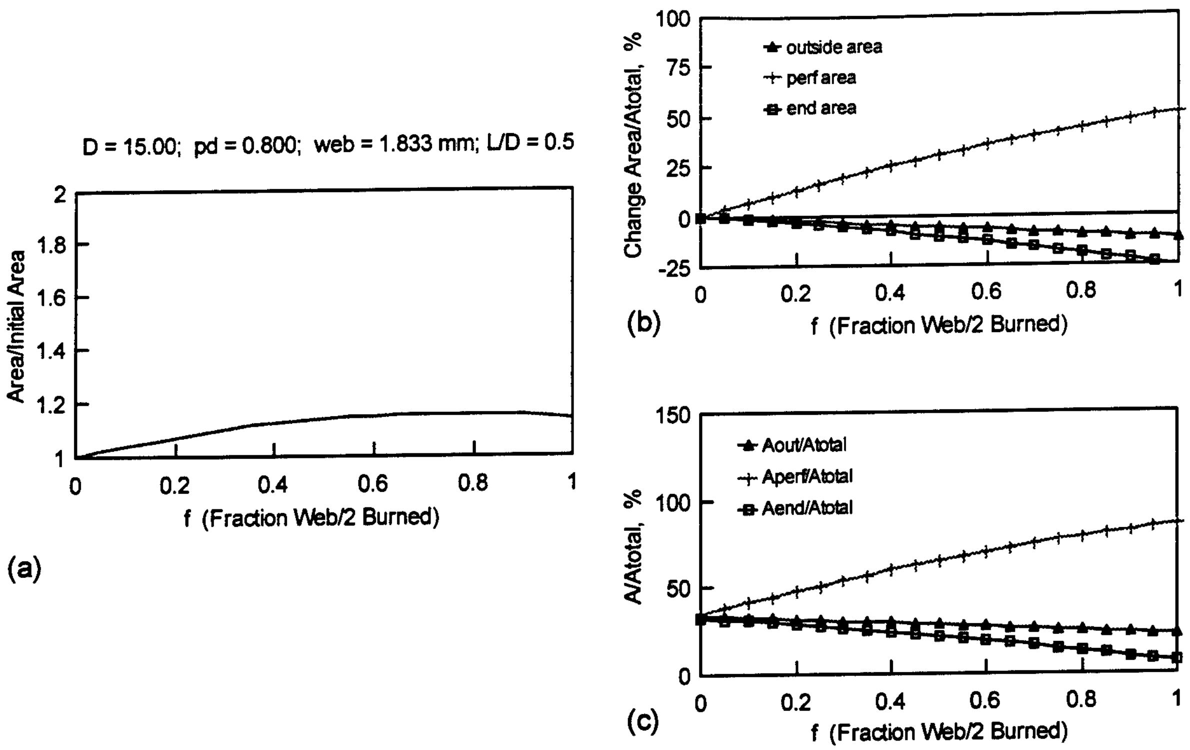

Figure 7. (a) Progressivity, 19-perf, L/D =0.5; (b) percent change in area; (c) areas, percent of original.

achieve the highest progressivity. The dependance is nonlinear, and not much improvement is realized beyond 3 or 4. With a small D/pd it is seen that the progressivity of the 19-perf grain is lower than the 7-perf grain. Moreover, the percent that will burn in a regressive manner after slivering is larger, making the overall progressivity even smaller. Calculations were done in which the contribution from the ends were removed (see the row marked "a" in Table 1), such as might be the case if the ends were inhibited from ignition or combustion or in the case where the grain is very long. The resulting progressivity for the 19-perf geometry is given by equation 9. For the 7-perf grain, the progressivity is given by

$$P_7 = 1.5f(D/pd - 3)/(D/pd + 7). \qquad (10)$$

The last row (b) in Table 1 illustrates the progressivity of the perforations alone. This would be the case if both the ends and outside surface were inhibited from ignition and combustion. The analytical expression for this is the same for any number of perforations (1, 7, or 19), is given by

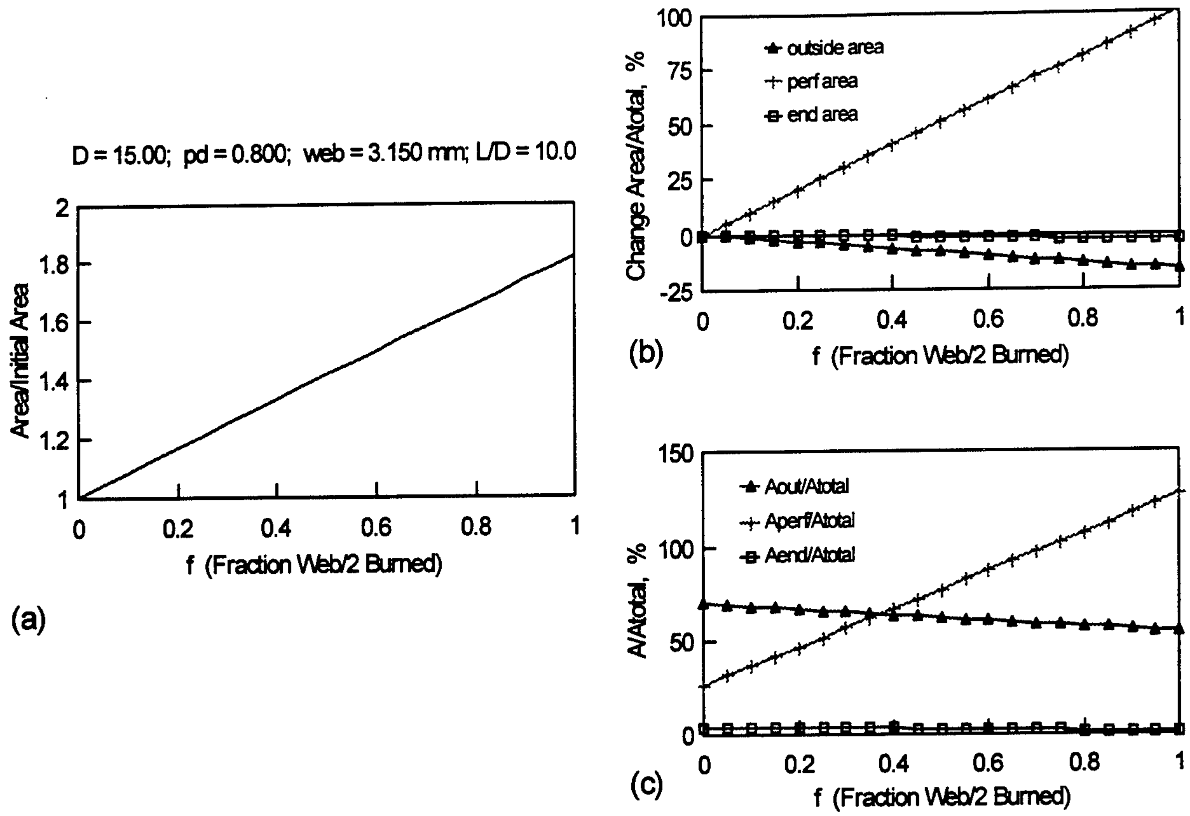

Figure 8. (a) Progressivity, 7-perf, L/D = 10; (b) percent change in area; (c) areas, percent of original.

$$P(\text{perforation}) = 1 + (f \times \text{web})/\text{pd}, \tag{11}$$

and is completely determined by the web/pd ratio. As is seen from Table 1(b), significant progressivities can be achieved if inhibitors could be successfully used on the regressive outside surfaces. However, it is also seen that percent propellant burning with that high progressivity is relatively low compared with the other table entries.

The importance of the geometrical effects of grain geometry can be illustrated with reference to the work of Robbins, Keys, and Brant (to be published). A new high-energy propellant was to be considered in the 120-mm cannon. The burn rate was lower than for the conventional JA2 propellant. Optimization calculations were carried out with the IBHVG2 interior ballistics code with

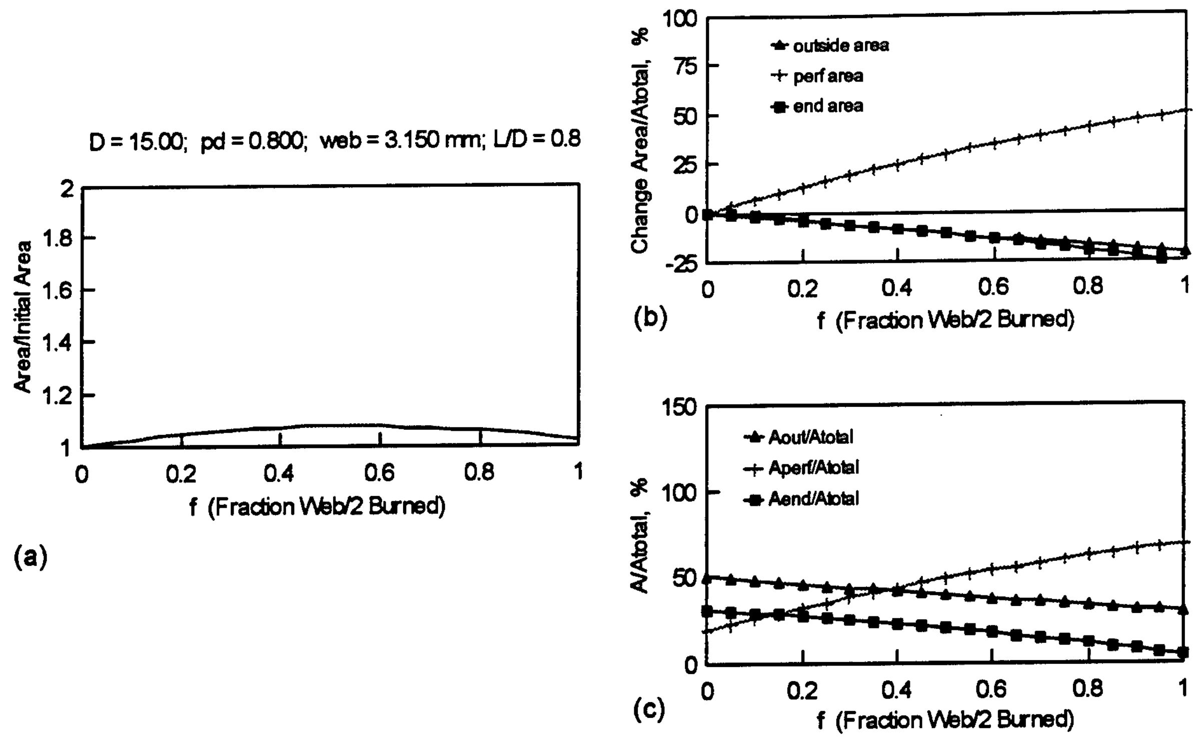

Figure 9. Progressivity, 7-perf, L/D = 0.8; (b) percent change in area; (c) areas, percent of original.

the new formulation. Since the new burn rate was lower, the propellant surface area had to be increased so as to achieve the required maximum pressure. This constraint resulted in a smaller web and grain diameter. For practical manufacturing considerations the perforation size was kept the same as for the JA2 formulation. As a consequence, the D/pd of the resulting grain was considerably smaller than for the JA2 propellant, which led to a significant reduction in progressivity. This resulted in a lower efficiency, and the expected performance was not achieved.

Another example of this is the study carried out by White et al. (1995) on the performance improvement to be expected in a 120-mm cannon by increasing the propellant loading density. The calculations (IBHVG2) were performed by incrementally increasing the loading density and then optimizing the grain web for maximum performance. It was found that at the high loading densities, the performance actually decreased mainly due to the fact that the surface area of the total charge had

Table 1. Progressivity and Percent Burned at Slivering

	19-Perf, D/pd = 8 at Slivering		7-Perf, D/pd = 8 at Slivering		19-Perf, D/pd = 15 at Slivering		7-Perf, D/pd = 15 at Slivering		19-Perf, D/pd = 30 at Slivering		7-Perf, D/pd = 30 at Slivering	
L/D	Prog.	% Burned	Prog.	% Burned	Prog.	% Burned	Prog.	% Burned	Prog.	% Burned	Prog.	% Burned
0.5	1.02	74	0.76	88	1.1	84	0.72	91	1.21	87	0.7	92
0.8	1.12	72	0.97	86	1.34	82	1.01	89	1.57	85	1.05	90
1	1.16	72	1.05	85	1.43	81	1.13	88	1.72	84	1.2	90
2	1.24	71	1.26	84	1.63	80	1.43	87	2.07	83	1.57	88
3	1.27	71	1.33	83	1.71	80	1.54	87	2.21	83	1.72	88
4	1.28	70	1.37	83	1.75	80	1.61	87	2.29	83	1.81	87
5	1.29	70	1.39	83	1.78	80	1.65	86	2.33	82	1.86	87
6	1.3	70	1.41	83	1.79	80	1.67	86	2.36	82	1.9	87
7	1.31	70	1.42	83	1.81	80	1.69	86	2.39	82	1.92	87
8	1.31	70	1.43	83	1.82	80	1.71	86	2.4	82	1.94	87
9	1.31	70	1.44	82	1.82	80	1.72	86	2.42	82	1.96	87
10	1.31	70	1.45	82	1.83	80	1.73	86	2.43	82	1.97	87
[a]	1.33	70	1.5	82	1.88	79	1.82	85	2.53	82	2.09	86
[b]	1.5	53	2.25	50	2.67	56	4	48	5.17	55	7.75	46

[a] Neglect contribution from grain ends.
[b] Perforations only burning.

to be decreased, meaning an increase in grain diameter and web. This resulted in a grain that could not be burned up before muzzle exit. When a grain length of 16.18 mm was used, the muzzle velocity calculated was 1,294 m/s, with 58% of the propellant consumed (D/pd = 48). The optimized web led to an L/D of 0.58. Using the same mass of propellant, the grain length was increased to 55.8 mm. The optimized calculation gave a muzzle velocity of 1,409 m/s with 76% of the propellant consumed (L/D = 2.42; D/pd = 41). Thus, for high energy and high loading density configurations, the progressivity can have significant effects on performance and should be considered in any performance calculations.

4. CONCLUSIONS

With the desire to go to higher energy/loading density propelling charges, calculations have shown the requirement of higher progressivity (chemical or geometrical) charges for efficient use of added energy (White et al. 1995). To achieve this for conventional geometry propellants, the calculations performed here have shown that for 7- and 19-perf grains the progressivity is improved by increasing the ratio of grain diameter to perf diameter to as large a value as is possible. The minimum size of the perforation is limited due to manufacturing difficulties. Additionally, Ruth et al. (1991) have shown the problems that arise if the ratio of grain length to perf diameter becomes too large. Pressures can build up within the perforations, causing grain rupture.

An additional value that should be maximized is the ratio of grain length to grain diameter. This aids in minimizing the regressive effects of the grain ends. The example given in section 3 showed that when the L/D ratio chosen was too small, there was an 8% loss in velocity. Again, there are limitations on just how large an L/D can be chosen because of the possibility of grain rupture. The progressivity dependence on L/D is very nonlinear, and a practical minimum value is between 1 and 2. Beyond this, the gain in progressivity is not large.

Calculations also demonstrated that very large gains in progressivity can be achieved if both the grain ends and outside surface could be inhibited from ignition and combustion. The resulting grain would have only perforations burning. It was also seen that, in this case, the progressivity did not depend on the number of perforations, only on the ratio of web to perf diameter.

In all this discussion concerning propellant grain progressivity, it should be pointed out that there is a ballistically negative effect on propelling charge temperature sensitivity due to high progressivity. The details of this have been discussed at length by Anderson and Puhalla (1991). Briefly, the physical effect can be described as follows. When the propellant is conditioned at different temperatures, the burn rate changes. As an example, suppose the propelling charge is conditioned to a low temperature and subsequently fired in a cannon. The burn rate will be lower, and, hence, the propellant will regress a smaller distance in a given time. If the progressivity is fairly large, as for a 19-perf propellant, the surface area will also be smaller as the propellant will be at a smaller fraction burned. As is seen in Figure 2 this will result in a smaller surface area. This will act as a negative feedback on the mass generation rate and will reduce the pressure even further. If the progressivity is neutral, as in a 1-perf grain, the feedback from the surface area into the mass generation rate will not be changed as the surface area does not change (or changes only slightly) for this neutral burning geometry. Hence, for propelling charges employing the 1-perf geometry, there will be a smaller effect on the ballistics due to a different operating temperature. Numerous examples of this for a variety of geometries are given by Anderson and Puhalla (1991).

A further liability of high-progressivity grain geometry is that the gun performance in terms of muzzle velocity and peak pressure becomes more sensitive to grain geometry variability that might occur during manufacture (Anderson and Puhalla 1991). This will be particularly important in a howitzer, where repeatability of performance is of critical importance.

INTENTIONALLY LEFT BLANK.

5. REFERENCES

Anderson, R. D., and R. T. Puhalla. "Temperature Sensitivity in Artillery Charge Design." BRL-TR-3206, U.S. Army Ballistic Research Laboratory, Aberdeen Proving Ground, MD, February 1991.

Juhasz, A. A., F. W. Robbins, R. E. Bowman, O. J. Doali, and W. P. Aungst. "Effects of Perforation L/d Ratio and Slotting On Stick Propellant Combustion." BRL-TR-2602, U.S. Army Ballistic Research Laboratory, Aberdeen Proving Ground, MD, October 1984.

Robbins, F. W. and A. W. Horst. "A Simple Theoretical Analysis and Experimental Investigation of Burning Processes for Stick Propellant." BRL-MR-03295, U.S. Army Ballistic Research Laboratory, Aberdeen Proving Ground, MD, July 1983a.

Robbins, F. W. and A. W. Horst. "Continued Study of Stick Propellant Combustion Processes." BRL-MR-03296, U.S. Army Ballistic Research Laboratory, Aberdeen Proving Ground, MD, July 1983b.

Robbins, F. W. and D. A. Worrell. "Fast Core Layered Propellant Study." <u>29th JANNAF Combustion Subcommittee Meeting</u>, vol. 1, CPIA Pub. 593, pp. 91–98, October 1992.

Robbins, F. W., T. Keys, and A. L. Brant. "Ramifications of Low Burn Rates on Gun Propellant Charge Design." Technical Report, U.S. Army Research Laboratory, Aberdeen Proving Ground, MD, to be published.

Ruth, C. R., F. W. Robbins, T. C. Minor, and A. A. Koszoru. "A New High-Progressivity/High-Density Propulsion Concept: Partially Cut Multiperforated Stick Propellant." BRL-TR-3189, U.S. Army Ballistic Research Laboratory, Aberdeen Proving Ground, MD, March 1991.

White, K. J., W. F. Oberle, A. A. Juhasz, I. C. Stobie, K. Nekula, G. L. Katulka, and S. Driesen. "Electrothermal-Chemical (ETC) Propulsion with High Loading Density Charges." ARL-TR-845, U.S. Army Research Laboratory, Aberdeen Proving Ground, MD, 1995.

INTENTIONALLY LEFT BLANK.

APPENDIX A:

GRAIN PARAMETERS FOR DETERMINING PROGRESSIVE OR REGRESSIVE SURFACES

INTENTIONALLY LEFT BLANK.

The expressions for evaluating the three different surface areas of a propellant grain are given by

$$A_o(\text{outside}) = \pi(D - 2r)(L - 2r), \tag{1}$$

$$A_p(\text{perforation}) = \pi(pd + 2r)(L\text{-}2r)n, \tag{2}$$

and

$$A_e(\text{ends}) = \pi/2[(D - 2r)^2 - n(pd + 2r)^2], \tag{3}$$

where r is the depth burned,

$$r = f(\text{fraction burned})\text{x web}/2. \tag{4}$$

OUTSIDE AREA

To determine if the surfaces are progressive or regressive during the course of burning, we take the derivative with respect to r. For the outside lateral surface we have

$$dA_o/dr = \pi[8r - 2(L + D)]. \tag{5}$$

This surface will be regressive when

$$dA_o/dr = \pi[8r - 2(L + D)] < 0 \tag{6}$$

or

$$r < (L + D)/4. \tag{7}$$

The relationship between web and diameter, D, is given by

$$D(\text{19-perf}) = 5pd + 6\text{web} \tag{8}$$

and

$$D(7\text{-perf}) = 3pd + 4web. \quad (9)$$

The maximum value of r will be web/2, which, from the definition of web for 7- or 19-perf grains (equations 8 and 9), will always be less than D/8. Consequently, equation 7 will always be true, and the outside lateral surface will always be regressive.

PERFORATION AREA

The perforation surfaces are progressive if the final area, A_{pf}, at burnout is greater than the initial area, A_{pi}. This can be expressed as

$$A_{pf} - A_{pi} > 0, \quad (10)$$

where

$$A_p = \pi(pd + 2r)(L-2r)n, \quad (11)$$

and for the initial surface r = 0,

$$A_{pi} = \pi n(pd)L, \quad (12)$$

and the final surface at slivering is r = web/2,

$$A_{pf} = \pi n(pd \times L - web \times pd + web \times L - web^2). \quad (13)$$

Evaluating equation 10 with 12 and 13,

$$L - pd > web. \quad (14)$$

For the 7-perf grain geometry (equation 9),

$$web = D/4 - 3pd/4. \quad (15)$$

Equation 14 becomes

$$L/D > 0.25 + 0.25pd/D. \tag{16}$$

Since the pd cannot be more than 1/3D (Figure 1), the value of pd/D for a 7-perf grain will range from 0 to a maximum of 0.333. Consequently, for the perforation surfaces to be progressive,

$$L/D > 0.3333. \tag{17}$$

It is clear that the perforation surfaces will be progressive for most practical grain geometries. Some examples of the progressivity of the perforation surfaces of a 7-perf grain for various values of L/D are given in Figure A-1.

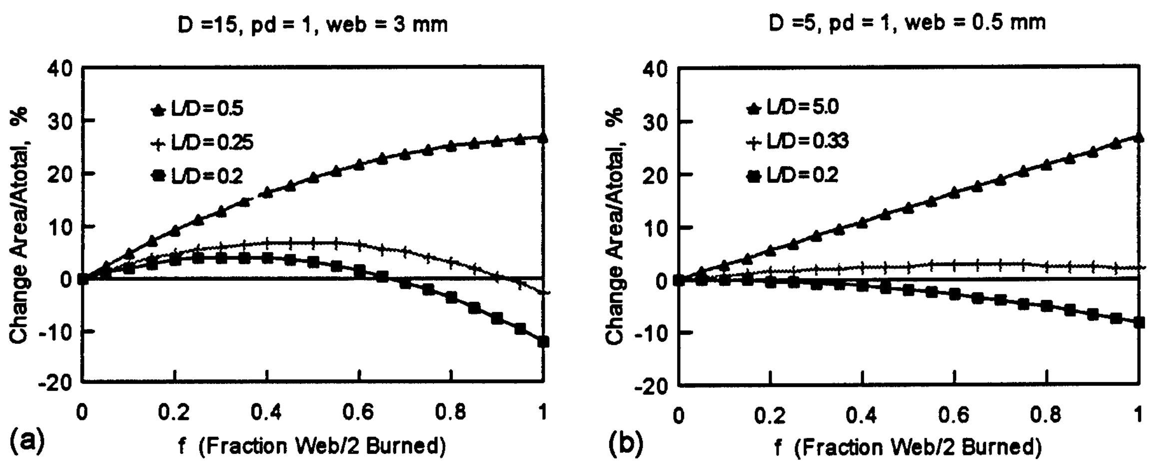

Figure A-1. Percent perforation area change, 7-perf grain; (a) pd/D = 0.0667, (b) pd/D = 0.2.

For the 19-perf grain geometry (equation 8),

$$web = D/6 - 5pd/6. \tag{18}$$

Equation 14 becomes

$$L/D > 0.167 + 0.167pd/D. \quad (19)$$

The value of pd/D for a 19-perf grain will range from 0 to a maximum of 0.2 (Figure 1). Consequently for the perforation surfaces to be progressive,

$$L/D > 0.2. \quad (20)$$

As was true for the 7-perf grain, for most practical designs the perforation surfaces will be progressive. Some examples of the progressivity of the perforation surfaces of a 19-perf grain for various values of L/D are given in Figure A-2.

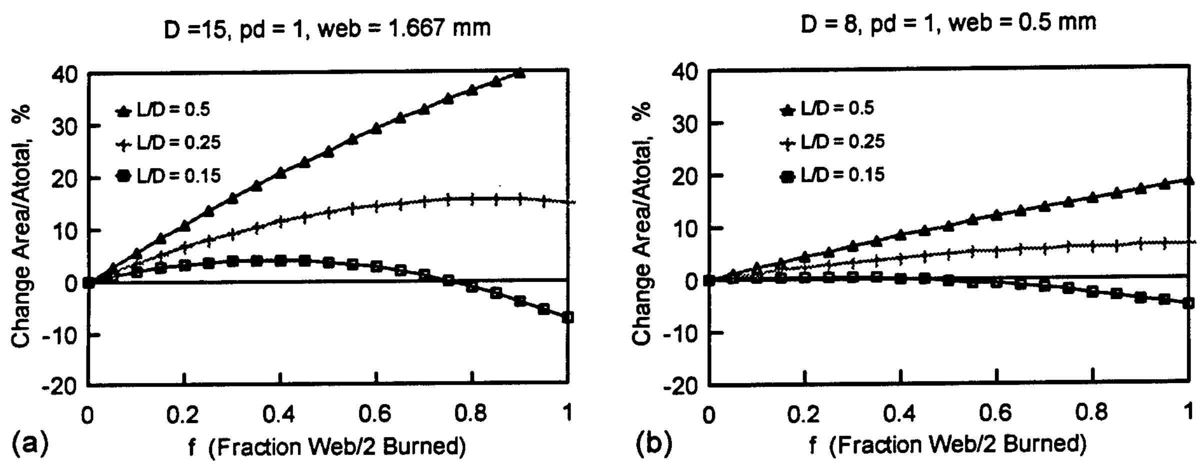

Figure A-2. Percent perforation area change, 19-perf grain; (a) pd/D = 0.067, (b) pd/D = 0.125.

END AREAS

The end areas will be regressive if, from equation 3, derivative with respect to r is less than zero,

$$dA_e/dt = \pi/2[-4(D - 2r) - 4n(pd + 2r)] < 0, \quad (21)$$

and

$$D + pd > 2r(1 - n). \quad (22)$$

From equation 22 it is clear that the right hand side will be less than zero for n = 7(-perf) or n = 19(-perf) propellants, and, consequently, the end areas will be regressive during the burning of the propellant.

INTENTIONALLY LEFT BLANK.

APPENDIX B:

DESCRIPTION AND LISTING OF SPREADSHEET PROGRAM USED FOR CALCULATING AREAS

INTENTIONALLY LEFT BLANK.

Calculations and graphs given in this report were carried out in a spreadsheet program using Lotus 1-2-3 Release 4 for Windows. A sample of a calculation with the resulting spreadsheet output is given on page 30. The program works in the following way: the grain parameters, defined in succeeding text, are placed into the appropriate cells. Each column, representing an area or percentage, is automatically updated. Graphs of the data (Figures 4–9) are automatically updated and then "copied" and "pasted" into the text of this document. The grain dimension input parameters and the cell location within the spreadsheet are as follows:

Input	Cell	Output	Cell(s)
grain diameter, D (mm)............	J7	fraction of web/2, f................	Q7...Q27
perf diameter, pd (mm)............	K7	outside area............................	D7...D27
length/diameter, L/D................	L2	perf area................................	D7...D27
number of perfs, n (7 or 19)......	M7	ends area................................	H7...H27
		distance burned, r..................	R7...R27
		progressivity..........................	T7...T27
		mass fraction burned............	O7...O27
		web..	P11
		progressivity @ slivering.....	K15
		fraction burned @ slivering..	K20
		grain length, L......................	L7

Various other parameters plotted in the graphs in this report are defined in the column headings for columns A through T. The analytical expression for each area (column A, B, etc.), which starts in row 7, is given below the spreadsheet (A7 = .., B7 = ..., C7 = ..., etc.). Graphs of these data were defined by the relevant columns, i.e., the x-axis was defined by the fraction web burned, Q7...Q27, the y-axis (Aout/Atotal) defined by C7...C27, etc. Graph HEADINGS were defined by cell J9 so that input data would always be associated with each graph. As has been noted, only 7- and 19-perf geometries were considered in these calculations.

The example given on the next page has the following parameters:

D = 15 mm, pd = 1 mm, L/D = 2, and n = 19.

GRAIN PROGRESSIVITY

Row	A	B	C	D	E	F	G	H	I	J	K	L	M	N	O	P	Q	R	S	T
3–6	outside area Ao= (D-2r)*pi*(L- mm^2	outside change/ total %	Aout/Atotal %	perf area Ap=(pd+2r)* pi*(L-2r)*n mm^2	perf area change/ total %	Aperf/Atotal %	A ends = mm^2	Aends change/ total %	Aend/Atotal %	grain diameter D mm	L/D = 2 perf diameter pd mm	grain length L mm	number perfs n		fraction mass burned	web/2 19-perf mm	fraction burned to web n	burned distance r mm	total area Atotal=Ap+A Aends mm^2	area ratio Atotal/Ainitial
7	1413.72	0.00	40.07	1790.71	0.00	50.76	323.57	0.00	9.17	15	1	30	19		0.000	0.833333	0.000	0.000	3528	1.000
8	1401.96	-0.33	39.74	1934.54	4.08	54.83	314.48	-0.26	8.91						0.031		0.050	0.042	3651	1.035
9	1390.24	-0.67	39.41	2077.55	8.13	58.89	304.99	-0.53	8.64	D = 15.00; pd = 1.000; web = 1.667 mm; L/D = 2.0					0.063		0.100	0.083	3773	1.069
10	1378.57	-1.00	39.08	2219.73	12.16	62.92	295.10	-0.81	8.36	Area Changes, 19-Perf Cylindrical					0.096	0.833333	0.150	0.125	3893	1.104
11	1366.94	-1.33	38.75	2361.08	16.17	66.92	284.83	-1.10	8.07	15.00	1.000	30.00	19		0.130	1.667	0.200	0.167	4013	1.137
12	1355.36	-1.65	38.42	2501.60	20.15	70.91	274.16	-1.40	7.77	2.0					0.164		0.250	0.208	4131	1.171
13	1343.82	-1.98	38.09	2641.29	24.11	74.87	263.10	-1.71	7.46		progressivity				0.200	323.5736	0.300	0.250	4248	1.204
14	1332.32	-2.31	37.76	2780.15	28.05	78.80	251.65	-2.04	7.13		@ slivering				0.237		0.350	0.292	4364	1.237
15	1320.86	-2.63	37.44	2918.19	31.96	82.72	239.80	-2.37	6.80		1.634				0.275		0.400	0.333	4479	1.270
16	1309.45	-2.96	37.12	3055.39	35.85	86.60	227.56	-2.72	6.45						0.314		0.450	0.375	4592	1.302
17	1298.09	-3.28	36.79	3191.77	39.71	90.47	214.93	-3.08	6.09		fraction				0.354		0.500	0.417	4705	1.334
18	1286.76	-3.60	36.47	3327.31	43.55	94.31	201.90	-3.45	5.72		burned				0.395		0.550	0.458	4816	1.365
19	1275.49	-3.92	36.15	3462.03	47.37	98.13	188.49	-3.83	5.34		@slivering				0.437		0.600	0.500	4926	1.396
20	1264.25	-4.24	35.83	3595.92	51.17	101.93	174.68	-4.22	4.95		0.804				0.480		0.650	0.542	5035	1.427
21	1253.06	-4.55	35.52	3728.98	54.94	105.70	160.47	-4.62	4.55						0.523		0.700	0.583	5143	1.458
22	1241.91	-4.87	35.20	3861.21	58.69	109.44	145.88	-5.04	4.13						0.568		0.750	0.625	5249	1.488
23	1230.81	-5.18	34.89	3992.61	62.41	113.17	130.89	-5.46	3.71						0.613		0.800	0.667	5354	1.518
24	1219.74	-5.50	34.57	4123.18	66.11	116.87	115.51	-5.90	3.27						0.660		0.850	0.708	5458	1.547
25	1208.73	-5.81	34.26	4252.93	69.79	120.55	99.74	-6.34	2.83						0.707		0.900	0.750	5561	1.576
26	1197.75	-6.12	33.95	4381.84	73.44	124.20	83.57	-6.80	2.37						0.755		0.950	0.792	5663	1.605
27	1186.82	-6.43	33.64	4509.93	77.08	127.83	67.01	-7.27	1.90						0.804		1.000	0.833	5764	1.634

A7 = ($J$7-2*R7)*3.14159*($L$7-2*R7)

G7 = @IF($M$7=19,(3.1415*($J$7-2*R7)^2/2-9.5*3.14159*($K$7+2*R7)^2),(3.1416*($J$7-2*R7)^2/2-3.5*3.1416*($K$7+2*R7)^2))

B7 = 100*(A7-$A$7)/($A$7+$D$7+$G$7)

H7 = 100*(G7-$G$7)/($A$7+$D$7+$G$7)

K11 = @STRING(K7,3) P7 = +$P$10

C7 = 100*(A7/($A$7+$D$7+$G$7))

I7 = 100*(G7/($A$7+$D$7+$G$7))

L7 = +$L$2*$J$7

P10 = @IF($M$7=19,($J$7-5*$K$7)/12,($J$7-3*$K$7)/8)

D7 = ($K$7+2*R7)*3.14159*($L$7-2*R7)*$M$7

J9 = +"D = "&J11&"; pd = "&K11&"; web = "&P11&" mm; L/D = "&J12

L11 = @STRING(L7,2) P11 = @STRING(2*P7,3)

E7 = 100*(D7-$D$7)/($A$7+$D$7+$G$7)

J10 = +"Area Changes, "&M11&"-Perf Cylindrical"

M11 = @STRING(M7,0)R7 = +Q7*$P$7

S7 = +D7+A7+G7

F7 = 100*(D7/($A$7+$D$7+$G$7))

J11 = @STRING(J7,2)

K15 = T27

K20 = $O$27

T7 = S7/$S$7

J12 = @STRING(L2,1)

P13 = @IF($M$7=19,(3.1415*$J$7*$J$7/2-9.5*3.14159*($K$7+2*R7)^2),(3.1416*$J$7*$J$7/2-3.5*3.1416*($K$7+2*R7)^2))

O7 = IF($M$7=19,(1-($L$7-2*R7)*(($J$7-2*R7)^2-19*($K$7+2*R7)^2)/($J$7^2*$L$7-19*($K$7)^2*$L$7)),(1-($L$7-2*R7)*(($J$7-2*R7)^2-7*($K$7+2*R7)^2)/($J$7^2*$L$7-7*($K$7)^2*$L$7)))

Graphs are automatically keyed to columns. Graph headings are keyed to cell J9. J10-M11 are used in J9 and are updated for each data input change.

GRAIN PROGRESSIVITY; INPUT PARAMETERS, Diameter, D (J7), pd(perf diameter), (K7), L/D (L2) and either 7 or 19 perfs (M7).

NO. OF COPIES	ORGANIZATION
2	DEFENSE TECHNICAL INFORMATION CENTER DTIC DDA 8725 JOHN J KINGMAN RD STE 0944 FT BELVOIR VA 22060-6218
1	HQDA DAMO FDQ DENNIS SCHMIDT 400 ARMY PENTAGON WASHINGTON DC 20310-0460
1	CECOM SP & TRRSTRL COMMCTN DIV AMSEL RD ST MC M H SOICHER FT MONMOUTH NJ 07703-5203
1	PRIN DPTY FOR TCHNLGY HQ US ARMY MATCOM AMCDCG T M FISETTE 5001 EISENHOWER AVE ALEXANDRIA VA 22333-0001
1	PRIN DPTY FOR ACQUSTN HQS US ARMY MATCOM AMCDCG A D ADAMS 5001 EISENHOWER AVE ALEXANDRIA VA 22333-0001
1	DPTY CG FOR RDE HQS US ARMY MATCOM AMCRD BG BEAUCHAMP 5001 EISENHOWER AVE ALEXANDRIA VA 22333-0001
1	DPTY ASSIST SCY FOR R&T SARD TT T KILLION THE PENTAGON WASHINGTON DC 20310-0103
1	OSD OUSD(A&T)/ODDDR&E(R) J LUPO THE PENTAGON WASHINGTON DC 20301-7100

NO. OF COPIES	ORGANIZATION
1	INST FOR ADVNCD TCHNLGY THE UNIV OF TEXAS AT AUSTIN PO BOX 202797 AUSTIN TX 78720-2797
1	USAASA MOAS AI W PARRON 9325 GUNSTON RD STE N319 FT BELVOIR VA 22060-5582
1	CECOM PM GPS COL S YOUNG FT MONMOUTH NJ 07703
1	GPS JOINT PROG OFC DIR COL J CLAY 2435 VELA WAY STE 1613 LOS ANGELES AFB CA 90245-5500
1	ELECTRONIC SYS DIV DIR CECOM RDEC J NIEMELA FT MONMOUTH NJ 07703
3	DARPA L STOTTS J PENNELLA B KASPAR 3701 N FAIRFAX DR ARLINGTON VA 22203-1714
1	SPCL ASST TO WING CMNDR 50SW/CCX CAPT P H BERNSTEIN 300 O'MALLEY AVE STE 20 FALCON AFB CO 80912-3020
1	USAF SMC/CED DMA/JPO M ISON 2435 VELA WAY STE 1613 LOS ANGELES AFB CA 90245-5500
1	US MILITARY ACADEMY MATH SCI CTR OF EXCELLENCE DEPT OF MATHEMATICAL SCI MDN A MAJ DON ENGEN THAYER HALL WEST POINT NY 10996-1786

NO. OF COPIES	ORGANIZATION
1	DIRECTOR US ARMY RESEARCH LAB AMSRL CS AL TP 2800 POWDER MILL RD ADELPHI MD 20783-1145
1	DIRECTOR US ARMY RESEARCH LAB AMSRL CS AL TA 2800 POWDER MILL RD ADELPHI MD 20783-1145
3	DIRECTOR US ARMY RESEARCH LAB AMSRL CI LL 2800 POWDER MILL RD ADELPHI MD 20783-1145
	ABERDEEN PROVING GROUND
4	DIR USARL AMSRL CI LP (305)

NO. OF COPIES	ORGANIZATION
1	COMMANDER US ARMY ARDEC AMSTA AR CCL A PAUL WYLUDA BUILDING 65N PICATINNY ARSENAL NJ 07806-5000
2	COMMANDER U S ARMY ARDEC AMSTA AR CCHT T NADIMIROFF PALATHINGAL BLDG 65 SOUTH PICATINNY ARSENAL NJ 07806-5000
1	COMMANDER USATACOM AMSTA-TBI STEVE HOFFMAN WARREN MI 48397-5000
1	COMMANDER US ARMY YPG STEYP MT EW JACK PETERS YUMA AZ 85365-6099
1	COMMANDING OFFICER NSWC CRANE DIVISION GREG DENNISON 5403 SOUTHSIDE DRIVE LOUISVILLE KY 40214-5000
1	DIRECTOR BENET LABORATORIES AMSTA AR CCB RT DR S SOPOK WATERVLIET ARSENAL NY 12189-4050
1	NASA AMES RESEARCH CENTER MR DAVID BOGNANOFF MAIL STOP 230-3 MOFFETT FIELD CA 94035-1000

NO. OF COPIES	ORGANIZATION
1	NAVAL WEAPONS STATION SEAL BEACH FALLBROOK DTCHMNT 514 D HAWLEY 800 SEAL BEACH BOULEVARD SEAL BEACH CA 90740-5000
1	NSWC ATTN G GRAFF G23 DAHLGREN VA 22448-5100
1	NSWC MR GUAN HSU BLDG 44 NSWC-DD SILVER SPRING MD 20903-5640
1	NSWC DAHLGREN DIVISION H DAY 17320 DAHLGREN ROAD DAHLGREN VA 22448-5100
1	NSWC INDIAN HEAD DIVISION MS S PETERS CODE 6210D INDIAN HEAD MD 20640
1	NSWC INDIAN HEAD DIVISION CT RICHMOND 10901 NEW HAMPSHIRE AVE SILVER SPRINGMD 20903-5640
1	US ARMY FSTC MR PAUL HUNTER 220 SEVENTH ST NE CHARLOTTESVILLE VA 22901
1	LLNL DR S W KANG L 140 PO BOX 808 LIVERMORE CA 94550
1	PNL MR ROGER GRAVES PO BOX 999 RICHLAND WA 99352

NO. OF COPIES	ORGANIZATION
1	SANDIA NATIONAL LABS MR DANIEL W BARNETTE ORG 1421 MS 1111 ALBUQUERQUE NM 87185-1111
1	SANDIA NATIONAL LAB DR KARL SVENSEN MAIL STOP 1135 PO BOX 5800 ALBUQUERQUE NM 87185
1	ADVANCED POWER TECHNOLOGY MR STEVE ADAMS 66 WEST STREET PITTSFIELD MA 01201
1	ADVANCED PROJECTS RSCH INCORPORATED HOMAS H SOBOTA 147 WARD STREET HIGHSTOWN NJ 08520
1	AEROJET ORDNANCE DIVISION ATTN MR RALPH IRWIN 9236 EAST HALL ROAD DOWNEY CA 90241
1	ALLIANT TECHSYSTEMS INC JIM KENNEDY MN11 2626 600 SECOND ST NE HOPKINS MN 55343-8384
1	ARES INC ANDREW KERTIS JR BLDG 818 FRONT STREET ERIC INDUSTRIAL PARK PORT CLINTON OH 43452-9399
1	ARMTEC DEFENSE PRODUCTS CO JIM KRUSHAT 85 901 AVENUE 53 COACHELLA CA 92236
1	GENCORP AEROJET PROPULSION DIVISION J G TOWNSEND P O BOX 13222 SACRAMENTO CA 95813-6000

NO. OF COPIES	ORGANIZATION
1	KLINE ENGINEERING CO MR ROY KLINE 7 FREDON GREENDEL ROAD NEWTIN NJ 07860-5213
1	LOCKHEED MARTIN DEFNS SYS DR GEORGE CHRISTOFF OP2 100 PLASTICS AVE PITTSFIELD MA 01201-3698
1	LOCKHEED MISSILE & SPACE CO DR SEAN SHEN ORG 8910 BLDG 157 1111 LOCKHEED WAY SUNNYVALE CA 94089-3504
1	LOCKHEED MARTIN DEFNS SYS MR JIM TALLEY ROOM 1309 LAKESIDE AVENUE BURLINGTON VERMONT 05401
1	LOCKHEED MARTIN MIS & SPACE MR K YEH DEPT 81-30 BUILDING 157 1111 LOCKHEED WAY SUNNYVALE CA 94089-3504
1	GENERAL DYNAMICS PRINCETON COMBUSTION RESEARCH LABS INC DR NEALE MESSINA 475 US HIGHWAY ONE MONMOUTH NJ 08852-9650
1	QUANTEX ENGINEERING INC PETER A HOCHSTEIN 64 PARK STREET TROY MI 48083
1	SAIC MR HARDY SCHREIBER 2109 AIR PARK ROAD SE ALBUQUERQUE NM 87106

NO. OF COPIES	ORGANIZATION
1	SCIENCE AND TECH DIV INST FOR DEFNS ANALYSES DR GERALD GILBERT 1801 N BEAUREGARD ST ALEXANDRIA VA 22311-1772
1	SOUTHWEST RSRCH INST MR DAVID LITTLEFIELD PO BOX 28510 SAN ANTONIO TX 78238
1	UNIV OF DAYTON RSRCH INST PATRICK BAKER 300 COLLEGE PARK DAYTON OH 45469-0182
1	THIOKOL ANDY HAALAND PO BOX 707 MS 243 BRIGHAM CITY UT 84302-0707
1	SAIC DR. REX RICHARDSON 10260 CAMPUS POINT DRIVE SAN DIEGO, CA 92121
1	SAIC DR. WOODWARD WAESCHE 1710 GOODRIDGEDRIVE MCLEAN VA 22102
2	ALLIANT TECHSYS/RADFORD W.J. WORRELL S.J. RITCHIE RADFORD ARMY AMMO PLNT RADFORD VA 24141
2	SAIC DR. C.C. HSIAO DR. FRED SU 10260 CAMPUS POINT DRIVE SAN DIEGO CA 92121
1	AEROJET CORP ED LIU PO BOX 13222 SCARAMENTO, CA 95813

NO. OF COPIES	ORGANIZATION
2	ASHWIN HOSANGADI SANDY DASH CRAFTECH COMBUSTION RESEARCH AND FLOW TECHNOLOGY, INC PO BOX 1150 DUBLIN, PA 18917
1	DR. IAN MCNAB INST FOR ADVANCED TECH THE UNIV OF TEXAS AT AUSTIN 4030-2 W. BRAKER LANE AUSTIN, TX 78759
4	UNITED DEFENSE LP AMIR CHABOKI RICHARD JOHNSON BRIAN ISLE JAHN DYVIK ARMAMENT SYSTEMS DIV 4800 EAST RIVER RD MINNEAPOLIS MN 55421 1498
2	THIOKOL GARY DIXON BOB WARDLE SCIENCE & ENGINERING PO BOX 707, M/S 230 BRIGHAM CITY, UT 54302-0707
1	AEROJET CORP ED LIU PO BOX 13222 SCARAMENTO, CA 95813
1	DR. LEE HARRIS AMSTA-AR-AEE-B B3124 PICATINNY ARSENAL, NEW JERSEY, 07806-5000
1	COMMANDER GIL GRAFF NSWC 17320 DAHLGREN RD DAHLGREN, VA 22448-5100

NO. OF COPIES	ORGANIZATION
	ABERDEEN PROVING GROUND
45	DIR USARL AMSRL WM P A HORST P KASTE E SCHMIDT AMSRL WM PA R ANDERSON A BRANT L CHANG T COFFEE J COLBURN P CONROY M DEL GUERCIO J DE SPIRITO S HOWARD A JUHASZ G KATULKA G KELLER D KOOKER C LEVERITT T MINOR M NUSCA W OBERLE S RAY T ROSENBERGER C RUTH MAJ M SMITH I STOBIE K WHITE (8 CPS) G WREN AMSRL WM PB M BUNDY D LYON P PLOSTINS D WEBB P WEINACHT A ZIELINSKI AMSRL WM PC D DEVYNCK J HEIMERL A KOTLAR AMSRL WM PD R LIEB S WILKERSON

NO. OF COPIES	ORGANIZATION
1	SNC INDUSTRIAL TECHNOLOGY INC MR PIERRE ARCHAMBAULT 5 MONTE DES ARSENAUX LE GARDEUR QUEBEC CANADA J5Z 2P4
1	PETER W FULLER 47 MADEIRA AVENUE BROMLEY KENT BR1 4AR ENGLAND
1	W J JURENS 62 FIDLER AVENUE WINNIPEG MANITOBA CANADA R3J2R7
1	BELCAN TECHNOLOGIES C/O MARTIN SIMARD 500 SHERBROOKE STREET W SUITE 970 MONTREAL CANADA H3A 3C6
1	OTO MELARA VIA VALDILOCCHI 15 19136 LA SPEZIA ITALY

INTENTIONALLY LEFT BLANK.

REPORT DOCUMENTATION PAGE

Form Approved
OMB No. 0704-0188

1. AGENCY USE ONLY (Leave blank)	2. REPORT DATE	3. REPORT TYPE AND DATES COVERED
	October 1997	Final, August 1996

4. TITLE AND SUBTITLE

Effect of Propellant Grain Dimensions on Progressivity

5. FUNDING NUMBERS

PR: 1L162618A1FL

6. AUTHOR(S)

Kevin J. White

7. PERFORMING ORGANIZATION NAME(S) AND ADDRESS(ES)

U.S. Army Research Laboratory
ATTN: AMSRL-WM-PA
Aberdeen Proving Ground, MD 21005-5066

8. PERFORMING ORGANIZATION REPORT NUMBER

ARL-TR-1532

9. SPONSORING/MONITORING AGENCY NAMES(S) AND ADDRESS(ES)

10.SPONSORING/MONITORING AGENCY REPORT NUMBER

11. SUPPLEMENTARY NOTES

12a. DISTRIBUTION/AVAILABILITY STATEMENT

Approved for public release; distribution is unlimited.

12b. DISTRIBUTION CODE

13. ABSTRACT *(Maximum 200 words)*

For high loading density propelling charges, propellant grain geometry design is employed to improve ballistic efficiency. Specifically, grains that have 7 and 19 and even 37 perforations are used. These grains all have progressive geometries, i.e., surface areas that increase as the propellant burns. This report studies the effect of grain dimensions on progressivities of the 7- and 19-perforation geometries. Calculations show that for maximum progressivity, the ratio of grain diameter to perforation diameter should be as large as practical. It is shown that small values can degrade potential gun performance. Calculations also show that the grain length-to-diameter ratio should be at least between 1 and 2 for maximum progressivity. This effect is very nonlinear, and values less than 1 are shown to reduce progressivity and gun performance significantly. High-progressivity geometries have, however, an undesirable effect on ballistic temperature sensitivity and yield an increased sensitivity to propellant manufacturing variability.

14. SUBJECT TERMS

propellants, grain geometry, progressivity, interior ballistics

15. NUMBER OF PAGES

38

16. PRICE CODE

17. SECURITY CLASSIFICATION OF REPORT	18. SECURITY CLASSIFICATION OF THIS PAGE	19. SECURITY CLASSIFICATION OF ABSTRACT	20. LIMITATION OF ABSTRACT
UNCLASSIFIED	UNCLASSIFIED	UNCLASSIFIED	UL

NSN 7540-01-280-5500

Standard Form 298 (Rev. 2-89)
Prescribed by ANSI Std. 239-18 298-102

INTENTIONALLY LEFT BLANK.

USER EVALUATION SHEET/CHANGE OF ADDRESS

This Laboratory undertakes a continuing effort to improve the quality of the reports it publishes. Your comments/answers to the items/questions below will aid us in our efforts.

1. ARL Report Number/Author ARL-TR-1532 (White) ____________ Date of Report October 1997 ______

2. Date Report Received ______________________________

3. Does this report satisfy a need? (Comment on purpose, related project, or other area of interest for which the report will be used.) ______________________________

4. Specifically, how is the report being used? (Information source, design data, procedure, source of ideas, etc.) ______

5. Has the information in this report led to any quantitative savings as far as man-hours or dollars saved, operating costs avoided, or efficiencies achieved, etc? If so, please elaborate. ______________________________

6. General Comments. What do you think should be changed to improve future reports? (Indicate changes to organization, technical content, format, etc.) ______________________________

CURRENT ADDRESS

____
Organization

____
Name | E-mail Name

____
Street or P.O. Box No.

____
City, State, Zip Code

7. If indicating a Change of Address or Address Correction, please provide the Current or Correct address above and the Old or Incorrect address below.

OLD ADDRESS

____
Organization

____
Name

____
Street or P.O. Box No.

____
City, State, Zip Code

(Remove this sheet, fold as indicated, tape closed, and mail.)

(DO NOT STAPLE)

DEPARTMENT OF THE ARMY

OFFICIAL BUSINESS

NO POSTAGE
NECESSARY
IF MAILED
IN THE
UNITED STATES

BUSINESS REPLY MAIL
FIRST CLASS PERMIT NO 0001,APG,MD

POSTAGE WILL BE PAID BY ADDRESSEE

DIRECTOR
US ARMY RESEARCH LABORATORY
ATTN AMSRL WM PA
ABERDEEN PROVING GROUND MD 21005-5066